Global Segmentation Algorithm for Partially Saturated Granular Geomaterials

Kokeb A. Abera, E.I.T., S.M. ASCE[1], Kalehiwot Nega Manahiloh, Ph.D., P.E., M. ASCE[2], and Mohammad Motalleb Nejad, S.M. ASCE[3]

[1] Graduate Student, Dept. of Civil and Environmental Engineering, University of Delaware, 301 DuPont Hall, Newark, DE 19716, U.S.A.; email: kabera@udel.edu.
[2] Corresponding Author, Assistant Professor, Dept. of Civil and Environmental Engineering, University of Delaware, 301 DuPont Hall, Newark, DE 19716, U.S.A.; email: knega@udel.edu; Phone: (302) 831-2495; Fax: (302) 831-3640.
[3] Graduate Student, Dept. of Civil and Environmental Engineering, University of Delaware, 301 DuPont Hall, Newark, DE 19716, U.S.A.; email: mohmtlb@udel.edu.

ABSTRACT

A new global segmentation technique, namely refined statistics-based method is proposed. X-ray computed tomography (CT) images of partially saturated granular geomaterials are segmented using this technique. Index properties of the geomaterials are quantified using the new technique and compared with those of the Otsu- and iterative-Otsu techniques. For the tested silica sand specimen, the new-technique-estimated void ratio and the degree of saturation were 0.67 and 39.35%. The estimates for the glass bead specimen yielded 0.64 and 43.49%, respectively. The true void ratio (0.66) and degree of saturation (37.71%) were determined with user controlled Image-Pro software package. It was found that the proposed method estimated the void ratio and the degree of saturation with 1.52 and 4.35 percent errors for the silica sand and with 15.63 and 0.34 percent errors for the glass bead, respectively. The computational time of the proposed method was found to be shorter than other methods considered. Overall, it is concluded that the proposed technique performed better in segmenting three-phase granular geomaterials.

Citation information: please cite this work as follows

Abera Kokeb, A., N. Manahiloh Kalehiwot, and M. Nejad Mohammad, *Global Segmentation Algorithm for Partially Saturated Granular Geomaterials*., in *IFCEE 2018*.

Link to published article: https://ascelibrary.org/doi/10.1061/9780784481585.046

INTRODUCTION

The process of separating areas of interest, patterns, or subsets of pixels with common features in an image is known as image segmentation (Liao *et al.* 2001). For images acquired via CT scanning, each pixel contains gray-level intensity information. Pixel intensities range from the weakest shade of gray (i.e., black) to the strongest shade of gray (i.e., white) (Madra *et al.* 2014). These values are then saved as an aggregate of bits and the possible range of intensities is dependent on the number of bits representing the image. For instance, for an 8-bit image, the intensity values vary from 0 to 255. In the case of this work, images of partially saturated granular geomaterials utilize three-phase segmentation to separate the gaseous-fluid, solid, and liquid-fluid phases, which may partially fill the pores.

Image segmentation techniques have undergone great advancement since the pioneering work of Brice and Fennema (1970). One such approach, histogram thresholding, introduces one or more intensity values to an intensity distribution (i.e., image histogram) of an image and separates the objects of interest (i.e., foreground) from the background. Depending on the constituent elements (i.e., phases) of an image, thresholding techniques could be bi-level or multi-level (Leedham *et al.* 2003). Bi-level thresholding techniques produce a two-phase segmented image by introducing one threshold value to the histogram (Kohler 1981; Pal and Pal 1993). On the other hand, multi-level thresholding techniques introduce more than one threshold value to the histogram (Kapur *et al.* 1985; Arora *et al.* 2008). Regardless of the approach, the number of segmented regions is always equal to the number of thresholds plus one.

Thresholding of images could be done at global or local scales. Global thresholding techniques use the statistical information of an intensity value distribution for the total pixels in a given image and local thresholding methods use the statistical information of a set of neighboring pixels to classify a pixel (Singh *et al.* 2011). While global thresholding techniques are generally easier to use for segmentation purposes, the main problem associated with these techniques is that the effects of noise (i.e., random variation in pixel intensity) cannot be eliminated by these methods (Leedham *et al.* 2003). However, global thresholding techniques provide sufficiently accurate results for the segmentation of images with clear distinct phases, as in the case with granular materials. Numerous global thresholding techniques such as Otsu's (1979) method have been proposed by several researchers. In the presented work, the concepts of Otsu's (1979) method are employed to modify the pre-existing technique and propose a new, three-phase segmentation technique.

One of the main benefits of using global segmentation techniques is avoiding the need for specialty software (e.g., Volume Graphics®, Image-Pro®, and Avizo®) that may not be readily, or easily accessible. In this study, a simple Gaussian filter is used for image enhancement. This filtering technique provided satisfactory enhancement results, although not as precise as more sophisticated filtering techniques such as edge detection based anisotropic diffusion (Perona and Malik 1990; Catte *et al.* 1992; Sheppard *et al.* 2004) and nonlocal means filter (Buades *et al.* 2005). For this work, void ratio and degree of saturation were chosen as benchmark parameters

for evaluating segmentation performance. In reality, it may be argued that other parameters, such as capillary pressure and permeability, may serve as more ideal benchmark parameters. However, this would require the usage of specialty software programs with pre-programmed pore-morphology analyzing capabilities, that of which was neither available nor the focus for this study.

REFINED STATISTICS-BASED THREE-PHASE THRESHOLDING

Otsu (1979) proposed one of the most widely used and oldest global thresholding techniques, where an optimal threshold value is selected as the pixel value located at a sharp valley between peaks representing the objects and background of an image's gray-level histogram (Otsu 1979). The basis of this technique separates the two classes by minimizing within-class variance and maximizing between-class variance for optimal threshold selection. In other words, the optimal threshold value is the pixel value that results in the minimized summation of the foreground and background spreads (Sahoo *et al.* 1988).

Equations 1-4 are used for Otsu's (1979) three-phase method, where the optimal threshold values (i.e., t1 and t2) are taken as the pixel values yielding the maximum value of Equation 4. Note that these four equations are first applied to the entire range of pixels represented by the gray-level histogram to obtain threshold one. Threshold two is then determined by applying the same four equations to a histogram ranging from the smallest pixel value to the value of threshold one.

$$mean = \frac{\sum_{i=1}^{m} i * f_i}{m} \quad (1) \qquad meanli = \frac{\sum_{i=1}^{t-1} i * f_i}{m} \quad (2) \qquad meangi = \frac{\sum_{i=t}^{m} i * f_i}{m} \quad (3)$$

$$t = \arg\max\{\sum_{i=1}^{t-1} f_i * \{meanli - mean\}^2 + \sum_{i=t}^{m} f_i * \{meangi - mean\}^2\} \quad (4)$$

In Equations 1-4 *m* stands for the highest possible pixel value in an image; *i* represents any pixel value between one and *m*; *f* represents frequency; mean, meanli, and meangi represent the means of pixel intensities ranging from one to *m*, one to *t*-1, and *t* to *m*, respectively; and *t* refers to the optimal threshold value of either t1 or t2.

Algorithms representing the modification and extension of Otsu's (1979) method, as well as the technique proposed here, were coded with MATLAB© (Mathworks 2015). Three of the techniques: Otsu (1979) three-phase, the iterative Otsu, and the refined statistics-based method, were modified for proper implementation in MATLAB©. For coding purposes, the range of grayscale pixel intensities for the analyzed 8-bit images is set between 1and 256, rather than 0 and 255. Void ratio was determined by dividing the number of void pixels by the number of solid pixels. Degree of saturation was determined by dividing the number of water pixels by the number of void pixels, expressed as a percentage. Since the scanned images represent a three-phase system, void pixels consist of water and air pixels.

As with the previous method, the iterative Otsu method calculates threshold one (t1) with Equations 1-4. The initial value for threshold two (t2) is calculated using Equations 5-7. The reason for expanding Otsu's (1979) three-phase method into the iterative Otsu method is because the procedure followed for finding the threshold two through Otsu's (1979) three-phase method does not necessarily result in the optimal value. Equations 8-10 determine a threshold value referred to as threshold new (tnew). Equations 8-10 are then used again in a loop (threshold new is assigned as threshold two) and the loop terminates once the value of threshold new is within two gray-level pixel values of the previous iteration. Once this criterion is met, the threshold new values will be assigned as the optimal value of threshold two.

$$mean1 = \frac{\sum_{i=1}^{t1} i * f_i}{\sum_{i=1}^{t1} f_i} \qquad (5)$$

$$mean2 = \frac{\sum_{i=t1+1}^{m} i * f_i}{\sum_{i=t1+1}^{m} f_i} \qquad (6)$$

$$t2 = \frac{(mean1 + mean2)}{2} \qquad (7)$$

$$mean3 = \frac{\sum_{i=1}^{t2} i * f_i}{\sum_{i=1}^{t2} f_i} \qquad (8)$$

$$mean4 = \frac{\sum_{i=t2+1}^{m} i * f_i}{\sum_{i=t2+1}^{m} f_i} \qquad (9)$$

$$tnew / t2 = \frac{(mean3 + mean4)}{2} \qquad (10)$$

Equations 11-12 represent the core equations in the algorithm of the refined statistics-based method. The optimal values of threshold one and two are assumed to lie to the left or right of the mean pixel intensity within unknown numbers of standard deviations. This proposed method follows a concept that numerous distributions have a tendency to follow the Dirac delta function with the peak located near the mean pixel intensity values (Arora *et al.* 2008). As mentioned in the work of Arora *et al.* (2008), many images contain normally distributed histograms. An estimation of such a distribution is a Gaussian distribution. Such distributions have high frequency values concentrated around the mean (μ). However, not all images have histograms with normal distributions. Fitting parameters, k1 and k2, are utilized in the segmentation of images with asymmetric or skewed histograms. Through alteration of the fitting parameters, the concepts applied for normally distributed histograms adapt to non-uniform distributions.

$$t1 = abs\left(\mu + \frac{\sigma * (k2 - k1)}{2}\right) \qquad (11)$$

$$t2 = abs\left(\frac{\sigma * (k1 + k2)}{2}\right) \qquad (12)$$

Arora *et al.* (2008) provides similar equations to those in Equations 11-12. In that work, one value was chosen for both k1 and k2 for simplicity. Arora *et al.* (2008) method does not provide successful segmented images for the geomaterials of this study when the values of k1 and k2 were kept equal. A parameter sensitivity analysis showed that the algorithm is more sensitive to changes in the values of k1 than k2. In this work, the values of k1 and k2 were carefully picked to ensure a segmentation that capture all portions of the raw image. For the geomaterials used in this study, it is recommended that k1 range from zero to two and that k2 range from zero to three, while ensuring that k2 is always greater than k1. The exact values taken by the fitting parameters vary depending on the type of images being analyzed. The proposed

method provides a faster processing time than both the Arora *et al.* (2008) and Otsu (1979) three-phase methods and a superior thresholding than the Otsu (1979) three-phase method.

The algorithm of the proposed segmentation method utilizes modified-statistical information, in comparison to the Arora *et al.* (2008), to provide higher-quality segmented images and faster processing time. The key difference in the image segmentation step between these two methods is that the Arora *et al.* (2008) method was tested on generic images whereas the proposed method was specifically created for analyzing geomaterials. As previously mentioned, the algorithm proposed by Arora *et al.* (2008) is capable of finding multiple thresholding values (as many as the user desires) to apply for image segmentation. However, in the presented work, it is specifically shown that modifying the Arora *et al.* (2008) algorithm leads to more reliable thresholds for three-phase geomaterials. In contrast to the Arora *et al.* (2008) method, a sensitivity analysis was conducted on the images of the geomaterials used in this study to recommend a range of values for the fitting parameters, k1 and k2. Adding restrictions to these values can significantly reduce processing time, lead to more accurate threshold selection, and improve segmentation.

RESULTS AND DISCUSSION

The three thresholding techniques described in the preceding section were applied to X-ray CT images obtained for silica sand and glass beads specimens. For presentation purposes, and for comparison of the performance of each thresholding technique, a typical slice of each image set is used. A standalone executable software program in which the aforementioned techniques were embedded was developed and deployed into a graphical user interface (GUI). In addition to its user-friendly environment, this application was packaged in such a way that MATLAB© software would not be required to perform the analyses. Prior to image segmentation, it is essential to crop the raw images into an exact area-of-interest (AOI). The images analyzed in this work were cropped using a circular AOI window, because the cross-sectional area of the specimens was circular. This approach ensures that pixels outside the AOI would not be included in the statistical analysis. The standalone software allows users to draw the cropping window on top of the opened X-ray image and save it. The same crop window can then be used to crop all of the remaining images.

The silica sand specimen was newly prepared in a laboratory setting with a diameter of 6.35 mm. X-ray CT scanning provided ninety-image slices for this specimen. In order to quantitatively verify the accuracy of the results of the three techniques, the void ratio and degree of saturation for this specimen were also determined with the image processing software, Image-Pro© (Media Cybernetics 2004). These values were found to be 0.66 and 37.71%, respectively. Figure 1 shows a typical silica sand slice with the applied manual crop as displayed in the standalone software developed as part of this study. Figure 2 shows, graphically, the use of the developed the refined statistics-based algorithm.

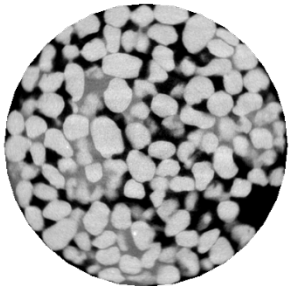

Figure 1. Typical segmented image: partially saturated silica sand specimen.

Figure 3 shows segmented images obtained from Otsu (1979) three-phase method, the iterative Otsu method, and the refined statistics-based method. The calculated void ratios were 0.88, 0.88, and 0.67, respectively. The two Otsu-based methods produced the same average threshold one value of 172. In this context, “average” refers to the average of threshold values calculated for all images in the set. The value for the degree of saturation varied with threshold two due to degree of saturation being a relationship between water and void pixels. Specifically for the Otsu-based methods, due to the number of solid pixels remaining the same, a lower threshold two value resulted in a higher degree of saturation and vice versa.

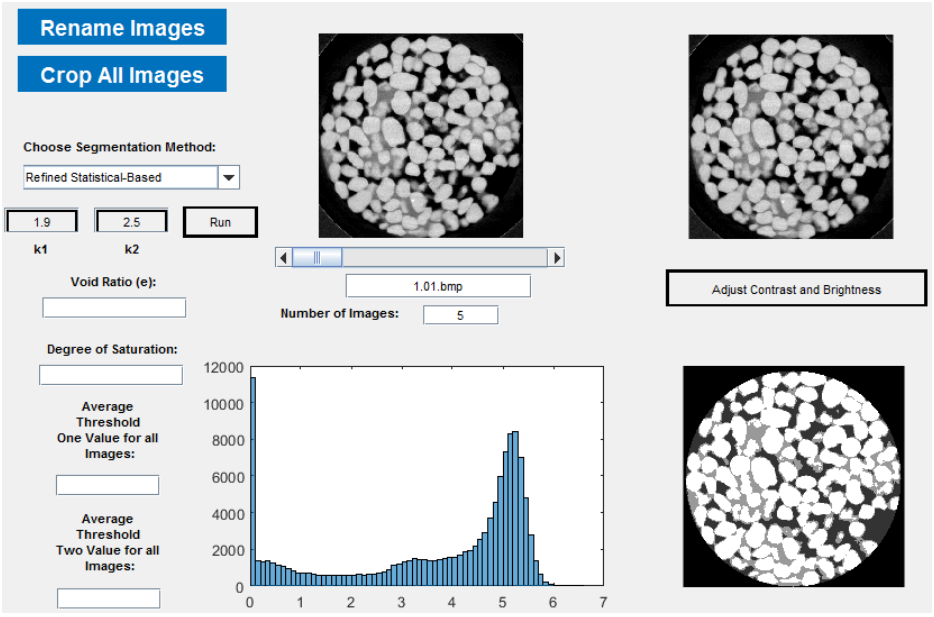

Figure 2. Partially saturated silica sand results of the refined statistics-based technique.

The degrees of saturation for Otsu (1979) three-phase method and the iterative Otsu method were determined as 16.94% and 41.45%, respectively. Quantitatively, these methods overestimated void ratio. This led to the solid particles in Figures 3a and 3b to be eroded. Otsu (1979) three-phase method greatly underestimated the degree of saturation with more than 50% error, as compared to the degree of saturation obtained from Image-Pro©. The iterative Otsu method slightly overestimated the degree of saturation, compared to Image-Pro, by approximately 10%. However, as observed in Figure 3b, the segmented silica sand specimen has pixels erroneously displayed as water pixels while not so in the original image slice.

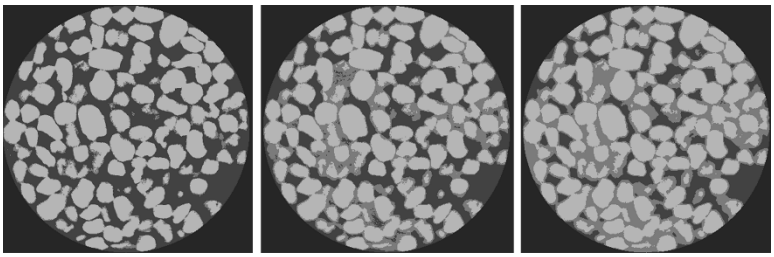

(a) (b) (c)

Figure 3. Segmented images of a partially saturated silica sand slice: (a) Otsu's (1979) three-phase method, (b) iterative Otsu method, (c) refined statistics-based method.

On average, the refined statistics-based method had the smallest threshold two value and a degree of saturation value of 39.35%. The k1 and k2 parameters for this method were chosen as 1.9 and 2.5, respectively. A trial-and-error process was utilized to obtain parameters that resulted in segmented images which effectively captured the three phases of the raw images. For this method, the average value of threshold one was found to be 158, indicating that more solid pixels and fewer void spaces were captured in the segmentation. By comparing the results of Figures 3a-3c, it is apparent that Figure 3c accurately contains more bridges of water between the solid particles and fewer voids within the solid particles, as seen in the original slice (Figure 1). Quantitatively, the void ratio and degree of saturation results of the proposed method are very close to the results of Image-Pro, with approximately 1.52% and 4.35% error, respectively.

The effectiveness of the proposed method was tested against the Arora *et al.* (2008) method while qualitatively keeping the segmentations the same (Figure 4). Note that the values of k1 and k2 differ between the methods since the role of these parameters in the algorithms are not the same. The proposed method was found to have a faster processing time than both the method of Arora *et al.* (2008) and Otsu (1979) three-phase methods. The proposed technique yielded approximately a 70% decrease in processing time than the Arora *et al.* (2008) method (1.73s rather than 5.79s). The same decrease was found between the proposed technique and Otsu (1979) (1.73s rather than 5.89s). For these reasons, the proposed method proved to be a refinement of the Arora *et al.* (2008) method.

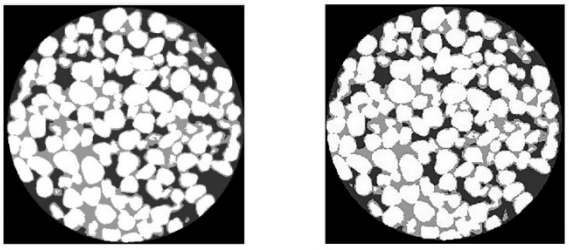

(a) (b)

Figure 4. Segmented unsaturated silica sand: (a) Arora *et al.* (2008), (b) refined statistics-based.

The glass bead specimen had a physical diameter of 10 mm. Ninety image slices, typical slice depicted in Figure 5, were obtained for this specimen through X-ray CT scanning. Figure 6

shows a result obtained by using the developed refined statistics-based algorithm on the glass bead specimen. Figure 7 presents the segmentation of a typical glass bead slice per thresholding technique. The Image-Pro void ratio and degree of saturation values were found to be 0.64 and 43.49%, respectively.

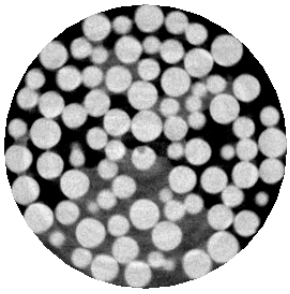

Figure 5. First cropped image slice of a partially saturated glass bead specimen.

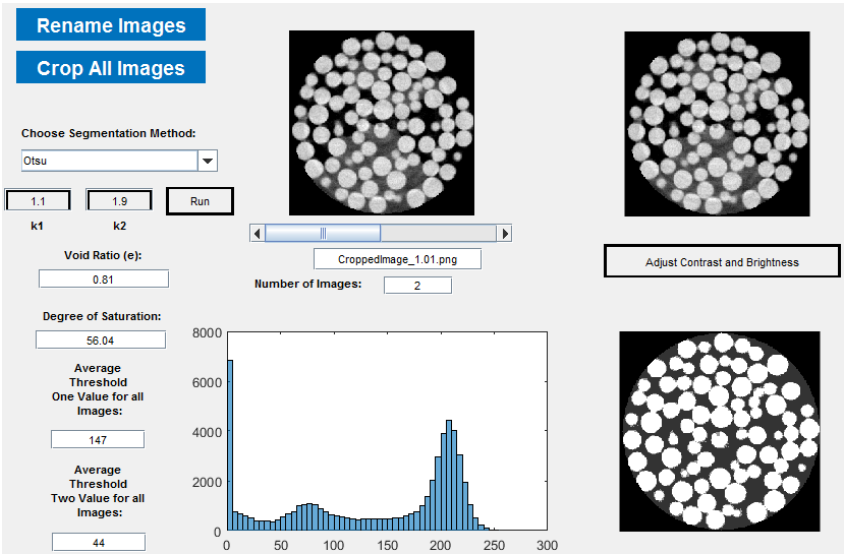

Figure 6. Partially saturated glass bead results of the refined statistics-based technique.

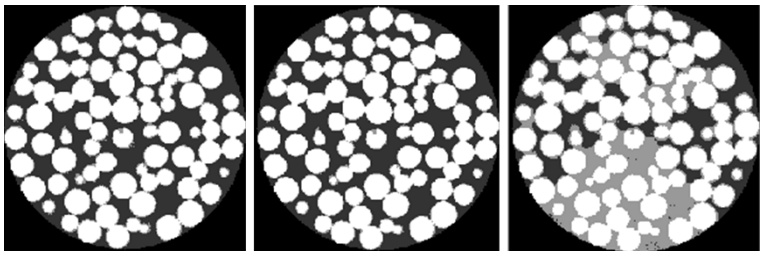

(a) (b) (c)

Figure 7. Segmented unsaturated glass bead: (a) Otsu's (1979) three-phase, (b) iterative Otsu, (c) refined statistics.

Following the same algorithmic trend as observed with the results of the silica sand specimen, Otsu's (1979) three-phase method and the iterative Otsu method yielded the same void ratio of 0.85 and average threshold one value of 159. Respectively, the degrees of saturation

were 14% and 15.26%. By analyzing Figures 7a and 7b, the segmentations failed to capture the majority of the water pixels seen in the original slice. This is due to the methods determining threshold two values that were too high. A higher threshold two-value results in a segmented image containing fewer water pixels and more air pixels, thus providing a lower degree of saturation.

Even though the iterative Otsu method did a slightly better job at capturing the water pixels than Otsu's (1979) three-phase method, the degree of saturation was still approximately three times smaller than the Image-Pro value. The void ratio and degree of saturation for the refined statistics-based method, with k1=1.35 and k2=1.75, were 0.74 and 43.64%, respectively. The proposed method's average threshold two value is more than two times smaller than those of the two techniques based on Otsu (1979). This decrease led to significantly more water pixels being captured, as visible in Figure 7c. Quantitatively, the degree of saturation of the proposed method was very accurately determined, in comparison to the Image-Pro value, with approximately 0.34% error. Calculated quantities that were discussed in preceding paragraphs are summarized and presented in Table 1.

Table 1. Summary of results

Method	Silica Sand				Glass bead			
	Void ratio	% Error	Degree of saturation	% error	Void ratio	% Error	Degree of Saturation	% Error
Image-Pro	0.66	0.00	37.71	0.00	0.64	0.00	43.49	0.00
Otsu	0.88	33.33	16.94	-55.08	0.85	32.81	14	-67.81
Iterative Otsu	0.88	33.33	41.45	9.92	0.85	32.81	15.26	-64.91
Refined statistics	0.67	1.52	39.35	4.35	0.74	15.63	43.64	0.34

The proposed technique yielded approximately an 84% decrease in processing time than the Arora *et al.* (2008) method (0.96s rather than 6.21s). An 80% decrease was found between the proposed technique and Otsu (1979) (0.96s rather than 4.92s). The segmentation of the glass bead specimen remained the same between the Arora *et al.* (2008) and proposed methods (Figure 8). Overall, the segmentation of the glass bead specimen was best captured by the refined statistics-based method.

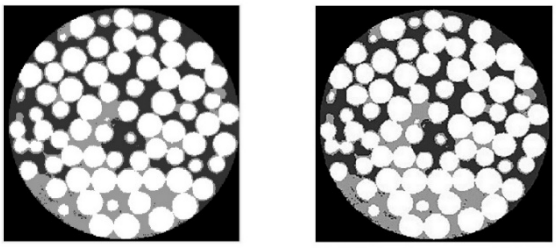

(a) (b)

Figure 8. Segmented images of a partially saturated glass bead: (a) Arora et al. (2008) method, (b) refined statistics-based method.

CONCLUSIONS

A refined statistics-based method was proposed and used to segment three-phase images of partially saturated silica sand and glass beads. Two other methods, Otsu's (1979) three-phase and the iterative Otsu, were utilized to test the performance of the proposed algorithm. The algorithms for the three thresholding techniques were coded into MATLAB© to determine void ratio and degree of saturation. The percent errors associated with the silica sand specimen showed that segmentation results were more heavily influenced by threshold two than threshold one. The reverse was found to be true for the glass bead specimen. Overall, the refined statistics-based method proved to be a successful technique for image segmentation. For the tested silica sand specimen, the new technique estimated the void ratio and the degree of saturation with 1.52 and 4.35 percent errors, respectively. The estimates for the void ratio of the glass bead specimen yielded a 15.63 percent error, whereas the degree of saturation had a low error of 0.34 percent. The freedom and flexibility allowed in the algorithm employed in this work, through allowing user input to adapt the algorithm, confirmed the superiority of the employed algorithm to those based on Otsu (1979). The work presented could well be integrated in morphology and cluster analysis and non-destructive materials characterization studies.

REFERENCES

Arora, S., Acharya, J., Vermac, A., and Panigrahi, P.K., 2008, "Multilevel thresholding for image segmentation through a fast statistical recursive algorithm," *Pattern Recognition Letters*, Vol. 29(2), 119-125.

Brice, C., and Fennema, C., 1970, "Scene analysis using regions," *Artificial Intelligence*, Vol. 1(3), 205-226.

Buades, A., Coll, B., and Morel, J., 2005, "Non-local algorithm for image denoising," *Proc. IEEE CVPR, 2005*.

Catte, F., Lions, P., Morel, J., and Coll, T., 1992, "Image selective and edge detection by nonlinear diffusion," *SIAM J. Numer. Anal.*, Vol. 29(1), 182-193.

Kapur, J.N., Sahoo, P.K., and Wong, A.K.C., 1985, "A New Method for Gray-Level Picture Thresholding Using the Entropy of the Histogram," *Computer Vision, Graphics, and Image Processing*, Vol. 29, 273-285.

Kohler, R., 1981, "A segmentation system based on thresholding," *Computer Graphics and Image Processing*, Vol. 15(4), 319-338.

Leedham, G., Yan, C., Takru, K., Joie, and Mian, L., 2003, "Comparison of some thresholding algorithms for text/background segmentation in difficult document images," 859-864.

Liao, P.S., Chen, T.S., and Chung, P.C., 2001, "A Fast Algorithm for Multilevel Thresholding," *Journal of Information Science and Engineering*, Vol. 17, 713-727.

Madra, A., Hajj, N.E., and Benzeggagh, M., 2014, "X-ray microtomography applications for quantitative and qualitative analysis of porosity in woven glass fiber reinforced thermoplastic," *Composites Science and Technology*, Vol. 95, 50-58.

Mathworks. 2015. Matlab 2015,Mathworks Inc., Natick, MA.

Media Cybernetics, 2004, "Image-Pro Plus Version 5.0. for Windows: Auto-Pro Reference, MAN AP 7846N00 20040229." Media Cybernetics, Silver Spring, MD.

Otsu, N., 1979, "Threshold Selection Method from Gray-Level Histograms," *IEEE Trans. Syst., Man Cybernetics*, Vol. SMC-9(1), 62-66.

Pal, N.R., and Pal, S.K., 1993, "A review on image segmentation techniques," *Pattern Recognition*, Vol. 26(9), 1277-1294.

Perona, P., and Malik, J., 1990, "Scale-space and edge detection using anisotropic diffusion," *IEEE Trans. Pattern Anal. Mach. Intel.*, Vol. 12(7), 629-639.

Sahoo, P.K., Soltani, S., and Wong, A.K.C., 1988, "A survey of thresholding techniques," *Computer Vision, Graphics, and Image Processing*, Vol. 41(2), 233-260.

Sheppard, A.P., Sok, R.M., and Averdunk, H., 2004, "Techniques for image enhancement and segmentation of tomographic images of porous materials," *Physica A: Statistical Mechanics and its Applications*, Vol. 339(1), 145-151.

Singh, T.R., Roy, S., Singh, O.I., Sinam, T., and Singh, K.M., 2011, "A new local adaptive Thresholding technique in Binarization," *International Journal of Computer Science Issues*, Vol. 8(2), 271-277.